ELSEVIER

Journal of Photochemistry and Photobiology A: Chemistry 148 (2002) 375–386

Journal of Photochemistry and Photobiology A:Chemistry

www.elsevier.com/locate/jphotochem

Photoelectrochemistry with the optical rotating disc electrode Part 4. Steady state and transient studies on colloidal CdS in the presence of solution phase photogenerated charge scavengers

Colin Boxall*

Centre for Materials Science, University of Central Lancashire, Preston PR1 2HE, UK

Received 24 July 2001; received in revised form 26 September 2001; accepted 26 September 2001

Abstract

Results are presented for the steady state and light-on transient photoelectrochemistry of two colloidal semiconductor/electron scavenger systems, CdS/$Fe(CN)_6^{3-}$ and CdS/MV^{2+}, studied with the optical rotating disc electrode (ORDE). Measurements with the ORDE allow calculation of values of 1.74×10^{-9} and 3.12×10^{-6} m s^{-1} for the electrochemical rate coefficient for reduction of $Fe(CN)_6^{3-}$ and MV^{2+}, respectively, at the photoexcited particle surface. The difference in the values of k_{ET} for the cationic and anionic scavenger species at the negatively charged CdS particles underlines the importance of the Coulombic interaction between particle and scavenger in determining the efficiency of particle-to-scavenger electron-transfer. ORDE measurements also indicate that the same Coulombic interactions are found to play an important role in determining the efficiency of the undesirable scavenger-to-particle back reaction, the reduced scavenger being oxidised by holes trapped at the particle surface. Importantly, the largest photocurrents are observed from the CdS/$Fe(CN)_6^{3-}$ system which also has the lowest value for the rate coefficient for the scavenger-to-particle back reaction. The value of ϕ, the quantum efficiency for the photogeneration of electrons detectable by the ORDE, is found to increase upon the addition of either scavenger. However, the low values of ϕ observed (0.027 for the CdS/$Fe(CN)_6^{3-}$ system, 0.02 for the CdS/MV^{2+} system) indicate that, even in the presence of an electron scavenger, the dominant processes within the particle are direct and indirect photogenerated electron–valence band hole recombination.

Keywords: Photoelectrochemistry; Photocatalysis; Colloidal semiconductors; Cadmium sulphide

1. Introduction

In our previous papers [1–3], we described the modelling of the light-on transient and steady state photocurrents exhibited at the optical rotating disc electrode (ORDE) by two general photophysical–chemical–electrochemical (PCE) systems.

1. The photophysical reversible chemical electrochemical (PRCE) process, wherein the photoexcited sensitiser S^* participates in a reversible chemical reaction with a charge scavenger, A, in solution, the products of which are oxidised at the electrode:

$$\text{solution :} \quad S \xrightarrow{h\nu} S^* \xrightarrow{k_0} S \tag{Ia}$$

$$\text{solution :} \quad S^* + A \xrightarrow{k_1} S^+ + A^- \xrightarrow{k_2} A \tag{Ib}$$

$$\text{electrode :} \quad A^- \rightarrow A + e^-, \qquad E^0_{A^-/A} \tag{Ic}$$

Reaction (Ib) may be considered as being chemically reversible with respect to A/A^-.

2. The photophysical irreversible chemical electrochemical (PICE) process, wherein S^* participates in an irreversible chemical reaction with a charge scavenger, A:

$$\text{solution :} \quad S \xrightarrow{h\nu} S^* \xrightarrow{k_0} S \tag{IIa}$$

$$\text{solution :} \quad S^* + A \xrightarrow{k_1} S^+ + A^- \tag{IIb}$$

$$\text{electrode :} \quad A^- \rightarrow A + e^-, \qquad E^0_{A^-/A} \tag{IIc}$$

This paper, the fourth in a series of four, describes the application of the results of our previous paper to experiments on photoexcited colloidal semiconductors performed in the presence of deliberately added solution phase charge scavengers.

Colloidal semiconductors are currently attracting substantial attention, especially in regard to their applications in photoelectrochemical energy conversion and environmental photocatalysis (see e.g. [4–13]), Q (quantum)-state systems

* Tel.: +44-1772-893530; fax: +44-1772-892996.
E-mail address: cboxall@uclan.ac.uk (C. Boxall).

1010-6030/02/$ – see front matter
PII: S1010-6030(02)00065-5

(see e.g. [11–18]) superhydrophilicity [5] and the understanding of the mechanisms underlying these modes of action. All of these reactions/systems rely upon the initial absorption of photons of energies greater than that corresponding to the semiconductor band gap to form conduction band electron–valence band hole pairs (e^-_{CB}, h^+_{VB}). These holes/electrons may subsequently recombine (reaction Ia/IIa) or diffuse to the particle surface where they may either reduce/oxidise particle lattice sites or undergo interfacial electron-transfer, reacting with a surface adsorbed substrate (static charge transfer), a species in solution (dynamic charge transfer), the solvent or catalysts deposited on the surfaces of the particles. Such reactions can be described in terms of an electrochemical model [19], an approach which finds greatest utility in those processes most dependent upon efficient interfacial electron-transfer, such as energy conversion and photocatalytic systems.

Direct electrochemical study usually involves particle-to-electrode precipitation; while mimicking particle environments found in most practical Q-state and energy conversion systems, this perturbs the (assumed) spherical diffusion fields and surface adsorption equilibria that obtain at particles in free solution, so affecting their interfacial electron-transfer efficiencies. Thus, there is a need for photoelectrochemical techniques capable of in situ, non-perturbative solution-phase study of interfacial charge transfer-reactions involving colloidal semiconductors and charge scavengers. The ORDE is such a technique.

Comparatively few studies have been published on the electrochemistry of colloidal semiconductors. Heyrovsky et al. [20–23] have examined the dark polarographic and cyclic voltammetric behaviour of a range of metal oxide colloids with mercury drop electrodes. Albery et al. [24,25] have previously reported polarograms recorded from colloidal TiO_2 and CdS with the ORDE in the dark and in the light, whilst we have measured and characterised the transient photocurrents generated by semiconductor colloids, so yielding information relating to photogenerated charge carrier kinetics [1,2]. Of greater utility would be a study of the steady state and transient photocurrents generated by colloidal semiconductor/charge carrier systems using the ORDE and stationary optical disc electrodes (ODEs) [1]. Such experiments would be expected to yield information pertaining to the interfacial electron-transfer kinetics of photogenerated charge carriers. However, to the best of our knowledge, this has not yet been done.

Thus, the paper will be primarily concerned with the use of the ORDE in the study of two commonly encountered colloidal CdS/electron scavenger systems: the CdS/$Fe(CN)_6^{3-}$ system, wherein the scavenger is anionic; and the CdS/1,1′-dimethyl-4,4′-bipyridinium (methyl viologen, MV^{2+}) system, wherein the scavenger is cationic. We have chosen to study CdS due to its stability, ease of preparation and its widespread use as both a model compound and in practical photoparticle systems. The E^0 values of the $Fe(CN)_6^{3-}$/$Fe(CN)_6^{3-}$ and MV^{2+}/$MV^{+\bullet}$ couples are 0.119 and −0.69 V, respectively. As the nearly pH-invariant flat band potential of CdS is ca. −0.9 V [26], the oxidised forms of both couples are thermodynamically capable of scavenging electrons from the particle conduction band or shallow traps at or near the particle surface (trapping times are <100 fs for CdS [27–30]). Each system is treated as follows. First we report the results of experiments to determine: (i) the rotation speed dependence of the steady state photocurrent; and (ii) the time dependence of the light-on transient photocurrent recorded at a stationary ODE for each system. We then use the form of these dependencies to determine which asymptotic mathematical descriptions of the time and rotation speed dependence of the photocurrent at the ORDE are appropriate for each semiconductor/scavenger pair. Finally, we use those mathematical descriptions to derive values of k_0, k_1 and k_2.

2. Experimental

Construction and theory of the ORDE have been described previously [1,3,31,32]. In summary, it consists of a quartz rod (radius in the range 1.5–2.1 mm) polished at both ends, one of which is coated with Sb-doped SnO_2 to form a transparent disc electrode. The light source was a Thorn A1/233, 250 W, 24 V quartz iodine projector lamp. Light from the lamp is brought to focus on the uncoated end of the quartz rod of the ORDE; it then passes through the conducting coating of the distal end and into solution. The electrode used during this study has an area of 6.52×10^{-6} m^2.

All solutions were freshly made with doubly deionised water (DDW) (resistivity >18 MΩ cm) and thoroughly purged with N_2 before use. All chemicals were of AnalaR or GPR grade and, where necessary, further purified by recrystallisation. Two batches of colloidal CdS were used in these experiments—colloids A and B. Both were prepared by the method of Grätzel and co-workers [33] as modified by Albery et al. [25]. Experiments on these particles were carried out in a sol containing 10 mM $KC1O_4$ and 10 mM sodium hexametaphosphate (HMP); the concentration of CdS was 5 mM. Experiments were conducted in the absence of added charge scavengers.

Particle diameters and diffusion coefficients were measured using a Malvern PCS100SM Photon Correlation Spectrometer incorporated into a Malvern Automeasure 4700SM system. Particle diameters were invariant over a period of months once an initial period of about a week had passed. Colloid A was found to have a mean diffusion coefficient, D_P, of 1.9×10^{-11} m^2 s^{-1}; that of colloid B was found to be 3.19×10^{-11} m^2 s^{-1}. Their mean radii, r_P, were found to be 12.4 and 6.8 nm, respectively. Colloid absorption coefficients were determined using a Hewlett-Packard 8451 A spectrophotometer.

Light intensities were measured with an *Applied Photophysics* integrating photodetector. Where appropriate, 10 nm band pass interference filters (Ealing IRI 25 mm) were used

to provide monochromated light. Light intensity was varied using Ealing neutral density filters. Transient photocurrent studies were performed by manual removal of the light shield situated at the underside of the projector lamp.

Unless otherwise stated, experiments were conducted using unattenuated white light in order to maximise the photocurrents obtained. The number of photons absorbed by the sols during white light experiments was calculated as follows. The high energy cut-off of the lamp occurs at $\lambda = 300\,\text{nm}$. At that wavelength, the value of $\varepsilon_{P,\lambda}c_P$ ($\varepsilon_{P,\lambda}$ the natural extinction coefficient of the particles, ($m^2\,mol^{-1}$) at λ, c_P the particle concentration ($mol\,m^{-3}$)) was typically $\sim 2700\,m^{-1}$, which was also the largest value obtained in the wavelength range absorbed by our sols. The slowest rotation rate used in our experiments, $1\,s^{-1}$, corresponds to a diffusion layer thickness, X_D, of the order of 10^{-5} m. Beer–Lambert calculations show that the intensity of light after it has passed through the diffusion layer, $I_{x=X_D}$ (in $mol\,m^2\,s^{-1}$), is 97.6% of that at the electrode surface, I_0. Thus, the light is virtually unattenuated as it traverses the diffusion layer, which is uniformly irradiated throughout. We may therefore obtain the number of photons absorbed by our CdS during white light experiments by integrating the product of I_0 and $\varepsilon_{P,\lambda}c_P$ over the wavelength range, giving a value of $I_0\varepsilon_{P,\lambda}c_P$ of 0.587 mol of photons $m^{-3}\,s^{-1}$. By a similar method, the flux of photons emerging into solution from the distal end of the ORDE in the wavelength range between the high energy cut-off of the lamp and the band gap of CdS is found to be 1.01×10^{-3} mol of photons $m^{-2}\,s^{-1}$. This may be taken to be numerically equal to I_0.

All electrochemical measurements were conducted at 298 K using a purpose built low current potentiostat powered by dry cells. All potentials were measured and reported with respect to the saturated calomel electrode (SCE). Unless stated otherwise, the working potential was 0.75 V versus SCE. This potential was found to be safely upon the mass transport-limited current plateau of the oxidation wave of all particles and electron scavengers used in this work. In all experiments, the reported photocurrent, $i_{h\nu}$, is equal to the current recorded under illumination minus that in the dark.

3. Results

The CdS/$Fe(CN)_6^{3-}$ and CdS/MV^{2+} systems studied below are found to behave in accordance with the PRCE process described by reaction 1. For the convenience of the reader, we will first summarise the findings of our previous three papers [1–3] that are of relevance to such systems when studied using the ORDE.

3.1. Summary of the steady state behaviour of PRCE systems at the ORDE

The behaviour of the PRCE system (reaction I) at the ORDE has been modelled using the following assumptions:

1. The light makes only a small perturbation to the concentration of S (in $mol\,m^{-3}$), thus not altering the dark current value significantly. This also means that the solution does not bleach and that the light has a Beer–Lambert profile given by
$$I = I_0 \exp(-\varepsilon_\lambda [S] x) \quad (1)$$
where I_0 is the flux of light at the electrode surface (mols of photons $m^{-2}\,s^{-1}$), ε_λ the absorption coefficient ($m^2\,mol^{-1}$) at wavelength λ (m or nm) and I the flux of light at a distance x (m) from the electrode.
2. The homogeneous loss reactions are (pseudo-) first-order with respect to [S*] and [A^-] ($mol\,m^{-3}$), with rate coefficients k_0 and k_2 (s^{-1}), respectively.
3. A is present in such large excess that: (i) [A] ($mol\,m^{-3}$) is uniform in the vicinity of S/S* and that the electron-transfer reaction is (pseudo-) first-order with respect to [S*] with rate coefficient k_1 (s^{-1}); (ii) the kinetics of electron-transfer between S* and A are fast compared to those of mass transport of S*.
4. The electron-transfer kinetics of S* and A^- at the electrode are extremely rapid so that the photocurrent is under either mass transport or photochemical kinetic control.

Using these assumptions and the boundary conditions $[S^*] = 0$ at $x = 0$ and as $x \to \infty$, solution, we have shown that the convective diffusion equation for A^- at a rotating ORDE is given by

$$D_A \frac{\partial^2[A^-]}{\partial x^2} + v_x \frac{\partial[A^-]}{\partial x} + \phi' I_0 \varepsilon_\lambda [S] \times \exp(-\varepsilon_\lambda [S] x) - k_2[A^-] = 0 \quad (2a)$$

where v_x and units thereof, have been defined previously [1–3], D_A the diffusion coefficient ($m^2\,s^{-1}$) of A/A^- and

$$\phi' = \left(\frac{k_1}{k_1 + k_0}\right)\phi \quad (2b)$$

where ϕ is the quantum efficiency for photogeneration of S*. The system has four characteristic lengths, all in meters:

the thickness of the diffusion layer :
$$X_D = 0.643\,W^{-1/2}\,\nu^{1/6}\,D_A^{1/3}$$

the thickness of the reaction layer : $$X_{k,2} = \left(\frac{D_A}{k_2}\right)^{1/2}$$

the thickness of the absorbance layer : $$X_\varepsilon = \frac{1}{\varepsilon_\lambda [S]}$$

the thickness of the hydrodynamic layer : $$X_H = \left(\frac{\nu}{2\pi W}\right)^{1/2}$$

where W is the rotation speed of the electrode (s^{-1}), ν the kinematic viscosity of the solvent ($m^2\,s^{-1}$).

It is worthwhile considering these lengths in the light of assumptions 1–4. Assumption 1 means that the light obeys a Beer–Lambert profile across all four layers. The thickness

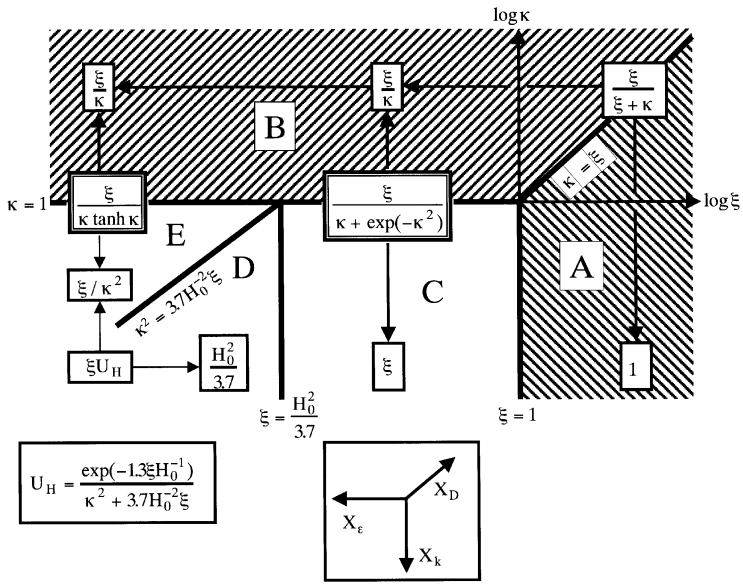

Fig. 1. Approximate solutions for the photoelectrochemical collection efficiency N_{hv} of PRCE systems, assuming that $\phi' = 1$. Different approximations hold for different values of ξ and κ_2 where ξ ($=X_D/X_\varepsilon$) compares the diffusion layer thickness to the distance over which the light is absorbed and κ_2 ($=X_D/X_{k,2}$) compares the thickness of the diffusion layer to the distance a photogenerated species diffuses before decomposing. The parameter H_0 ($=X_D/X_H$) compares the thickness of the diffusion layer to the thickness of the hydrodynamic layer. The 'signpost' shows how changes in X_ε, $X_{k,2}$ and X_D affect the position of the system on the diagram.

of the reaction layer $X_{k,2}$ is defined by the rate of the assumed (pseudo-) first-order loss reaction of A^- described in assumption 2. Finally, as described in assumption 4, the photocurrent is controlled by the time taken for A^- to diffuse across either X_D or $X_{k,2}$, whichever is the smaller.

Eqs. (2a) and (2b) may be solved by recasting in terms of the following dimensionless parameters:

$$H_0 = \frac{X_D}{X_H}, \qquad \xi = \frac{X_D}{X_\varepsilon}, \qquad \kappa_2 = \frac{X_D}{X_{k,2}}$$

and using the boundary conditions that $[A^-] = 0$ at $x = 0$ and as $x \to \infty$. It has proved useful to express the solution of Eqs. (2a) and (2b) in terms of a photoelectrochemical collection efficiency, N_{hv}, describing the recovery of the photogenerated A^- species at the electrode

$$N_{hv} = \frac{j_{A^-}}{I_0} \tag{3}$$

where j_{A^-} is the flux of A^- reaching the electrode, in mol m^{-2} s^{-1}. Fig. 1 shows the case diagram for the approximate solutions of N_{hv} derived from Eqs. (2) and (3) [1,31] assuming $\phi' = 1$. The solutions may be grouped into five cases, A–E, depending on the relative magnitudes of κ_2 and ξ. Table 1 summarises the rotation speed dependence of the steady state, mass transport-limited photocurrent, $(i_{hv})_L$, at the ORDE for each case.

3.2. Summary of the transient behaviour of PRCE systems at the ORDE

The stationary ODE is assumed to be illuminated by parallel light switched on at time $t = 0$, and which produces a concentration of S^* denoted by $[S^*]_t$ at t (in seconds). The scavenging of charge by A produces a measurable concentration of A^-, $[A^-]_t$. Using these assumptions and assumptions

Table 1
Summary of rotation speed dependence of steady state photocurrent, i_{hv}, for cases A–E of the PRCE system (adapted from [1,3])

Case	Dependence of i_{hv} on W	Parameters obtainable	Equation for i_{hv}	
A	Independent of W	ϕ'	$i_{hv} = FA\phi' I_0$	(4a)
B	Independent of W	$(\phi')^2/k_2$	$i_{hv} = FA\phi' I_0 \frac{X_{k,2}}{X_\varepsilon}$	(4b)
C	$i_{hv} \propto W^{-1/2}$	ϕ'	$i_{hv} = FA\phi' I_0 \frac{X_D}{X_\varepsilon}$	(4c)
D	Independent of W	ϕ'	$i_{hv} = FA\phi' I_0 \frac{H_0^2}{3.7}$	(4d)
E	$i_{hv} \propto W^{1/2}$	ϕ'/k_2	$i_{hv} = FA\phi' I_0 \frac{X_{k,2}^2}{X_\varepsilon X_D}$	(4e)

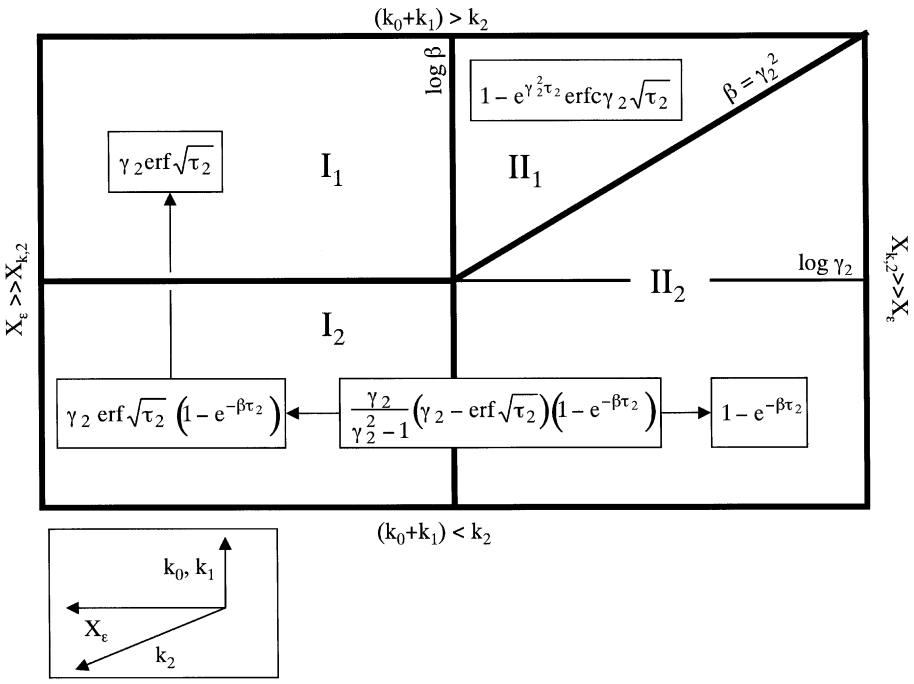

Fig. 2. Case diagram for the approximate solutions of Eq. (7). Different approximations hold for different values of β and γ_2, where β $(=(k_0+k_1)/k_2)$ compares the rate of loss of S* with the rate of loss of A^- and γ_2 $(=X_{k,2}/X_\varepsilon)$ compares the distance A^- diffuses before participating in a loss reaction with the distance over which the light is absorbed.

1–4, we have shown that the time-dependent convective diffusion equation for A^- at a *stationary* electrode is given by [3]:

$$\frac{\partial[A^-]_t}{\partial t} = D_A\frac{\partial^2[A^-]}{\partial x^2} + \phi' I_0\varepsilon_\lambda[S]\,e^{-\varepsilon_\lambda[S]x} \times (1-e^{-(k_1+k_0)t}) - k_2[A^-] \quad (5)$$

Eq. (5) may be solved by recasting in terms of the following dimensionless parameters:

$$\tau_2 = k_2 t \quad (6a)$$

$$\gamma_2 = \frac{X_{k,2}}{X_\varepsilon} \quad (6b)$$

$$\beta = \frac{k_0+k_1}{k_2} \quad (6c)$$

and using the boundary conditions that (i) at $x=0$, $[A^-]=0$ at all t; (ii) $[A^-]\to 0$ as $x\to\infty$ at all t; and (iii) $[A^-]=0$ at all x at $t=0$. Expressing the solution of Eq. (5) in terms of the time-dependent equivalent of the photoelectrochemical collection efficiency $N_{hv,t}$, gives

$$N_{hv,t} = \frac{\phi'\gamma_2}{\gamma_2^2-1}\left\{\gamma_2 - \text{erf}\sqrt{\tau_2} - \gamma_2\,e^{(\gamma_2^2-1)\tau_2}\,\text{erfc}(\gamma_2\sqrt{\tau_2})\right\} - \frac{\phi'\gamma_2}{\gamma_2^2-(1-\beta)}\left\{e^{-\beta\tau_2}\left[\gamma_2-\sqrt{1-\beta}\,\text{erf}\sqrt{(1-\beta)\tau_2}\right] - \gamma_2\,e^{(\gamma_2^2-1)\tau_2}\,\text{erfc}\left(\gamma_2\sqrt{\tau_2}\right)\right\} \quad (7)$$

Eq. (7) may be expressed as a group of less opaque, asymptotic solutions. These solutions for $N_{hv,t}$ are of greater analytical utility and are summarised in the case diagram of Fig. 2. The solutions may be grouped into four cases, I_1, I_2, II_1 and II_2, depending on the relative magnitudes of β and γ_2. Table 2 summarises the time dependence of the light-on transient photocurrent, $(i_{hv})_t$, recorded at a stationary ORDE for each case.

Table 2
Approximate analytical solutions for the transient and steady state photoelectrochemical collection efficiencies, N_{hv}, observed at a stationary ORDE from a PRCE system[a]

	Transient $N_{hv,t}$	Steady state N_{hv}	
Case I_1			
$\gamma_2 < 1$, $\beta > 1$	$\phi'\gamma_2$ erf $\sqrt{\tau_2}$	$\phi'\gamma_2$	(8a& b)
Case I_2			
$\gamma_2 < 1$, $\beta < 1$	$\phi'\gamma_2\,(1-e^{-\beta\tau_2})$ erf $\sqrt{\tau_2}$	$\phi'\gamma_2$	(9a& b)
Case II_1			
$\gamma_2 > 1$, $\beta > \gamma_2^2$	$\phi'\left(1-e^{\gamma_2^2\tau_2}\,\text{erfc}\left(\gamma_2\sqrt{\tau_2}\right)\right)$	ϕ'	(10a& b)
Case II_2			
$\gamma_2 > 1$, $\beta < \gamma_2^2$	$\phi'(1-e^{-\beta\tau_2})$	ϕ'	(11a& b)

[a] To obtain the corresponding photocurrent, multiply the relevant solution by FAI_0.

Thus, five cases fully describe the steady state photocurrents produced by a PRCE system at a rotating ORDE, while four cases fully describe the light-on transient photocurrents produced by the same system at a stationary electrode. We have shown that these steady state and transient cases may be more satisfactorily expressed in terms of 14 combined cases [3] that completely describe all of the cases presented in Figs. 1 and 2, specifically cases BI_1, BI_2, CI_1, CI_2, DI_1, DI_2, EI_1, EI_2, AII_1, AII_2, CII_1, CII_2 and EII_1, EII_2. Assignment of a system to a specific case is made on the basis of both the time and rotation speed dependence of the photocurrents observed at the ORDE and may be most readily accomplished by use of the flow diagram shown in Fig. 3. We shall use Fig. 3 to assign the CdS/$Fe(CN)_6^{3-}$ and CdS/MV^{2+} systems to their appropriate cases, and use the expressions for $N_{h\nu}$ and $N_{h\nu,t}$ associated with each case to derive values for ϕ, ϕ', k_0, k_1 and k_2 for each system.

3.3. The photoelectrochemistry of the colloidal CdS/$Fe(CN)_6^{3-}$ system

Photoelectrochemical control experiments were performed on solutions of ferricyanide in the absence of colloidal CdS. Upon illumination, despite ferricyanide possessing a broad absorption band centred at about 420 nm that is coincident with a significant amount of light output from the lamp, $Fe(CN)_6^{3-}$ was found to exhibit no intrinsic photocurrent activity over the wavelength range and at the light intensities employed in this work. Thus, any photocurrent enhancement found in the presence of colloidal CdS must be due to the interaction between ferricyanide and the photoexcited particles. Further, calculations indicate that, at the maximum concentration of ferricyanide used in the experiments described herein, the transmittance of light across the electrode diffusion layer or the ferricyanide reaction layer is greater than 99.7%. Thus, the light emerging from the electrode surface is practically unattenuated as it traverses either of these layers, allowing us to say that assumption 1 (vide supra) applies to A as well as S.

Fig. 4 shows plots of the mass transport-limited steady state photocurrent, $(i_{h\nu})_L$, versus $W^{-1/2}$ for CdS colloid A as a function of added $[Fe(CN)_6^{3-}]$. Fig. 5 shows plots of the light-on transient photocurrent, $(i_{h\nu})_t$, versus t as a function of added $[Fe(CN)_6^{3-}]$ for the same system. Following the procedures outlined in [2], the data recorded at $[Fe(CN)_6^{3-}] = 0$ in Fig. 5 can be used to calculate a value

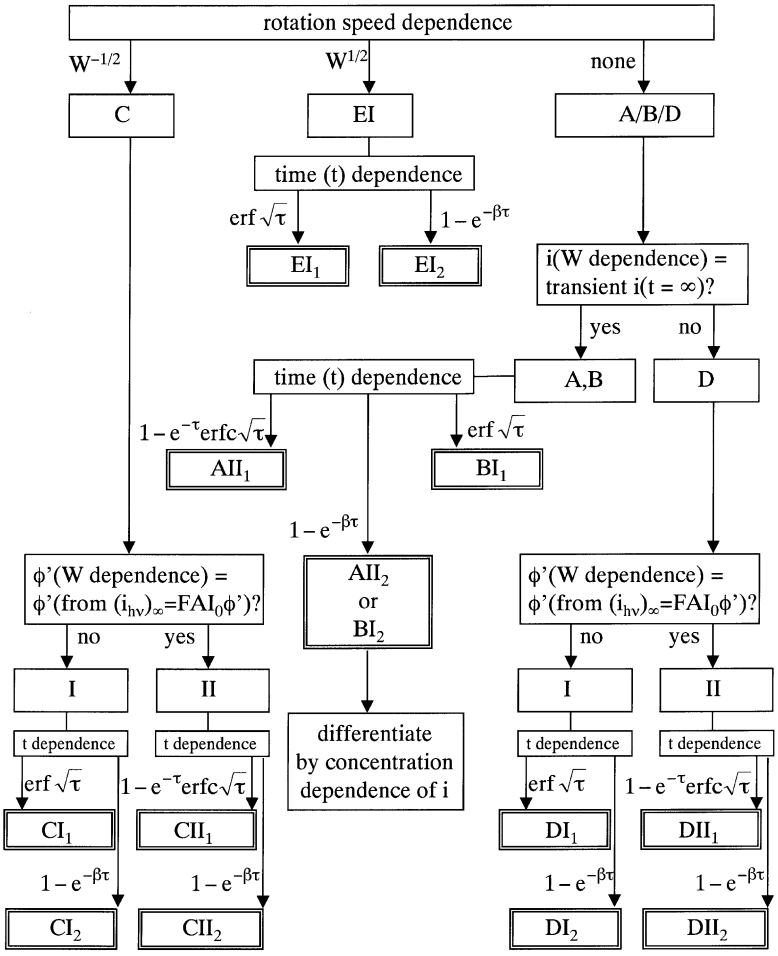

Fig. 3. Flow diagram summarising the protocol for PRCE case assignment.

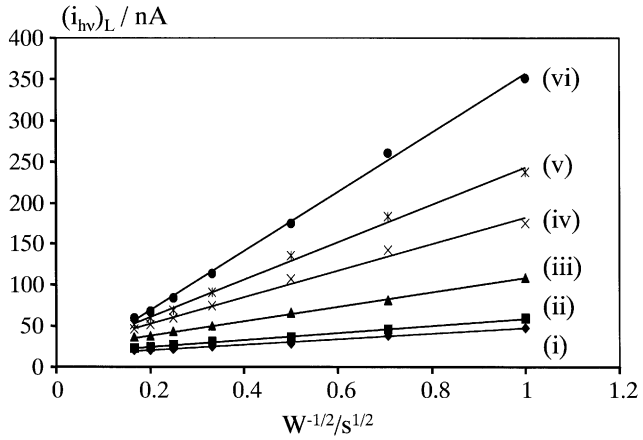

Fig. 4. Plots of mass transport-limited photocurrent, $(i_{hv})_L$ vs. $W^{-1/2}$ for CdS colloid A as a function of concentration of $[Fe(CN)_6^{3-}]$. $[Fe(CN)_6^{3-}] = 0$ (i); 7.7×10^{-4} (ii); 0.013 (iii); 0.025 (iv); 0.037 (v); and 0.093 mol m^{-3} (vi). [CdS] = 5 mol m^{-3}.

of k_0 of 0.091 s^{-1} for colloid A, which may then be used with the data recorded at $[Fe(CN)_6^{3-}] = 0$ in Fig. 4 to obtain a value of ϕ of 0.011.

The data in Figs. 4 and 5 can now be used to assign the CdS/$Fe(CN)_6^{3-}$ system to its appropriate case and so calculate values of k_1 and k_2. From Fig. 4, it can be seen that $(i_{hv})_L \propto W^{-1/2}$ under conditions where assumption 3 would be expected to hold, i.e. high $[Fe(CN)_6^{3-}]$. From this observation, Fig. 3 indicates that the system conforms to steady state case C and, necessarily, Eq. (4c), indicating that the photoreduced charge scavenger species are kinetically stable as they cross the diffusion layer of the electrode. Use of Eq. (4c) and $(i_{hv})_L$ versus $W^{-1/2}$ data from Fig. 4 recorded at $[Fe(CN)_6^{3-}] = 0.0933$ mol m^{-3} (where assumption 3 holds, vide infra) allows calculation of a value of ϕ' of 0.018. This value indicates that the main reaction for photogenerated electrons is recombination and that those surviving to participate in particle-to-scavenger electron-transfer do so because corresponding holes have been lost to particle corrosion reactions or trace adventitious electron donors [2].

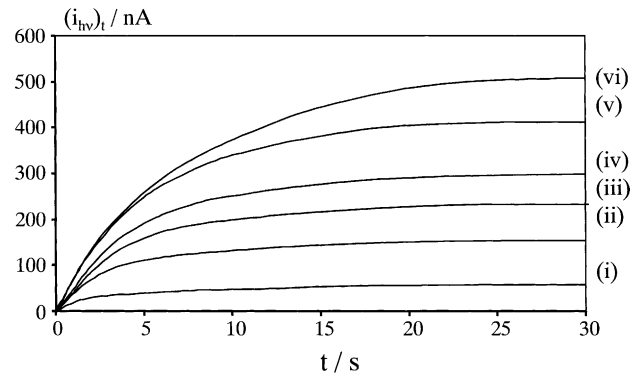

Fig. 5. Light-on current time transient for CdS colloid A at a stationary ODE as a function of $[Fe(CN)_6^{3-}]$. $[Fe(CN)_6^{3-}] = 0$ (i); 0.013 (ii); 0.025 (iii); 0.037 (iv); 0.0604 (v); and 0.093 mol m^{-3} (vi). [CdS] = 5 mol m^{-3}.

Fig. 3 can now be used to determine the transient sub-case of steady state case C to which the system conforms. Broadly speaking, the transient cases of Fig. 2 break down into two categories: those for which $\gamma_2 > 1$ where the transient current at near-steady state, $(i_{hv})_\infty$ is given by $FAI_0\phi'$ (Eqs. (10b) and (11b)); and those for which $\gamma_2 < 1$ where the transient current at near-steady state is given by $FAI_0\phi'\gamma_2$ (Eqs. (8b) and (9b)). Use of Eq. (10b) or (11b) to calculate ϕ' from the $(i_{hv})_\infty$ data of Fig. 5 recorded at $[Fe(CN)_6^{3-}] = 0.0933$ mol m^{-3} gives a value of ϕ' of 0.0008. This is significantly lower than the value of 0.018 obtained at the same $[Fe(CN)_6^{3-}]$ using Eq. (4c) and the data of Fig. 4, indicating that Eqs. (10b) and (11b) do not hold for this system. On the basis of this observation, Fig. 3 indicates that the light-on photocurrent behaviour of the CdS/$Fe(CN)_6^{3-}$ system conforms with transient case I, wherein $\gamma_2 < 1$ and $(i_{hv})_\infty$ is given by Eq. (8b)/(9b). Use of Eq. (8b)/(9b) in conjunction with $\phi' = 0.018$ and the $(i_{hv})_\infty$ data of Fig. 5 recorded at $[Fe(CN)_6^{3-}] = 0.0933$ mol m^{-3} then allows calculation of values of $X_{k,2}$ and k_2 of 7.6×10^{-5} m and 0.101 s^{-1}, respectively. As the slowest rotation rate used in these experiments, 1 s^{-1}, corresponds to a diffusion layer thickness, X_D, of 5.4×10^{-5} m for $Fe(CN)_6^{3-}$, which is again suggestive of the majority of the photoreduced charge scavenger species being kinetically stable as they cross the diffusion layer of the electrode.

From Eqs. (8b), (9b) and (2b) it can also be seen that, when assumption 3 holds:

$$\frac{1}{(i_{hv})_\infty} = \frac{X_\varepsilon}{\phi AFI_0 X_{k,2}}\left(1 + \frac{k_0}{k_1}\right) = \frac{X_\varepsilon}{\phi AFI_0 X_{k,2}}\left(1 + \frac{k_0}{k_1'[A]}\right) \quad (12)$$

where k_1' (m^3 mol^{-1} s^{-1}) is the second-order rate coefficient for the electron-transfer reaction between S* and A. Fig. 6 shows a plot of $(i_{hv})_\infty^{-1}$ versus $[Fe(CN)_6^{3-}]^{-1}$ derived from appropriate data from Fig. 5. From Eq. (12), a value of

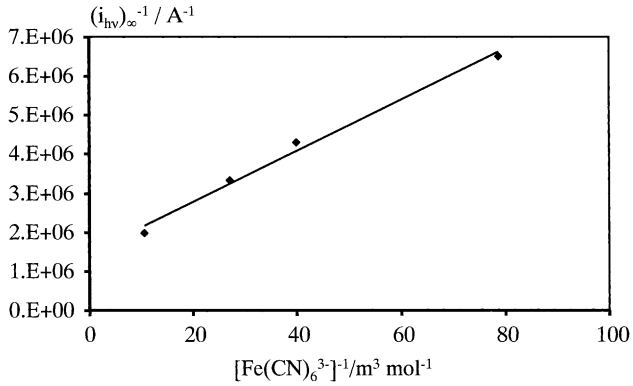

Fig. 6. Reciprocal steady state photocurrent recorded at a stationary ODE, $(i_{hv})_\infty^{-1}$, vs. $[Fe(CN)_6^{3-}]^{-1}$, plotted in accordance with Eq. (12) for that data of Fig. 5 recorded under conditions where assumption 3 is valid. [CdS] = 5 mol m^{-3}.

k_0/k_1' can be obtained when the slope of this plot is divided by its intercept. Using $k_0 = 0.091\,s^{-1}$ (vide supra) and the data of Fig. 6, k_1' is then found to be $2.029\,m^3\,mol^{-1}\,s^{-1}$, which corresponds to $k_1 = 0.189\,s^{-1}$ at $[Fe(CN)_6^{3-}] = 0.0933\,mol\,m^{-3}$.

Having obtained k_0, k_1 and k_2, it is now possible to identify which transient case, I_1 or I_2 the system conforms to in Fig. 2, and to compare the consequently predicted theoretical transient photocurrent behaviour with that observed experimentally. Differentiation between cases I_1 and I_2 can be most easily accomplished by consideration of the value of β (see Eq. (6c)) which, using the rate coefficient values determined above, is found to be 2.77 for the $CdS/Fe(CN)_6^{3-}$ system at $[Fe(CN)_6^{3-}] = 0.0933\,mol\,m^{-3}$. Used in conjunction with a calculated mean value of γ_2 of 0.044, this allows the system to be nominally assigned to case I_1. However, calculations indicate that the derived value of $\beta = 2.77$ is too close to $\beta = 1$ for the approximation given by Eq. (8a) in case I_1 to hold. Therefore, the theoretical transient photocurrent behaviour must be computed using a more accurate asymptotic expression for $(i_{hv})_t$ at $\gamma_2 < 1$, $\beta > 1$, given by Eq. (26c) of [3]:

$$(i_{hv})_t = FAI_0\phi' \left(\gamma_2 \operatorname{erf}\sqrt{\tau_2} - \frac{2\gamma_2}{\sqrt{(\beta-1)\pi}} e^{-\beta\tau_2} \int_0^{\sqrt{(\beta-1)\tau_2}} e^{\lambda^2}\,d\lambda\right) \quad (13)$$

The quality of the approximation provided by Eq. (13) may be clearly seen from Fig. 7 which shows both the experimental $(i_{hv})_t$ versus t plot recorded at $[Fe(CN)_6^{3-}] = 0.0933\,mol\,m^{-3}$ in Fig. 5 and the theoretical plot computed from Eq. (13) using the rate coefficient values derived above.

3.4. The photoelectrochemistry of the colloidal CdS/MV^{2+} system

As in the case of ferricyanide, in control experiments, MV^{2+} is found to possess no intrinsic photocurrent activity

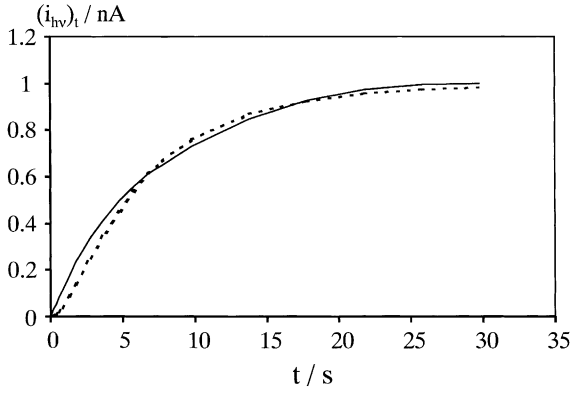

Fig. 7. Matching of experimental data (unbroken line) derived from the light-on transient photocurrent behaviour of CdS colloid A in the presence of $Fe(CN)_6^{3-}$ as an electron scavenger, to the theoretical curve (broken line) given by Eq. (13). [CdS] = $5\,mol\,m^{-3}$; $[Fe(CN)_6^{3-}] = 0.0933\,mol\,m^{-3}$.

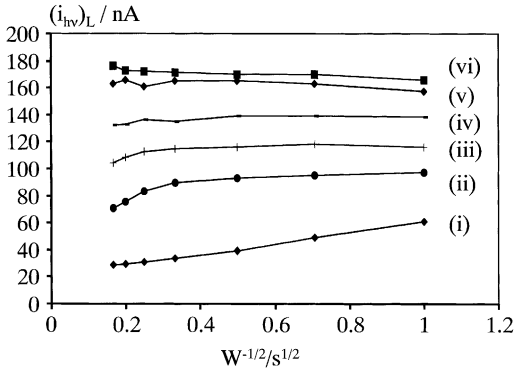

Fig. 8. Plots of mass transport-limited photocurrent, $(i_{hv})_L$ vs. $W^{-1/2}$ for CdS colloid B as a function of $[MV^{2+}]$. $[MV^{2+}] = 0$ (i); 0.99×10^{-4} (ii); 1.98×10^{-4} (iii); 3.38×10^{-4} (iv); 6.98×10^{-4} (v); and $9.09\times10^{-4}\,mol\,m^{-3}$ (vi). [CdS] = $5\,mol\,m^{-3}$.

over the wavelength range and at the light intensities employed in this work. Thus, any photocurrent enhancement found in the presence of colloidal CdS must be due to interaction between scavenger and photoexcited particles.

Fig. 8 shows plots of the mass transport-limited steady state photocurrent, $(i_{hv})_L$, versus $W^{-1/2}$ as a function of added $[MV^{2+}]$. Fig. 9 shows plots of the light-on transient photocurrent, $(i_{hv})_t$, versus t as a function of added $[MV^{2+}]$ for the same system. Following the procedures outlined in [2], the data recorded at $[MV^{2+}] = 0$ in Fig. 9 can be used to calculate a value of k_0 of $0.119\,s^{-1}$ for colloid B, in good agreement with the value of $0.091\,s^{-1}$ obtained for colloid A. This value of k_0 may then be used with the data recorded at $[MV^{2+}] = 0$ in Fig. 8 to obtain a value of ϕ for colloid B of 0.012, in excellent agreement with the value of 0.011 derived for colloid A.

The data in Figs. 8 and 9 can now be used to assign the CdS/MV^{2+} system to its appropriate case and so calculate values of k_1 and k_2. From Fig. 8, it can be seen that $(i_{hv})_L$ is independent of W under conditions where assumption 3 would be expected to hold, i.e. high $[MV^{2+}]$, and most

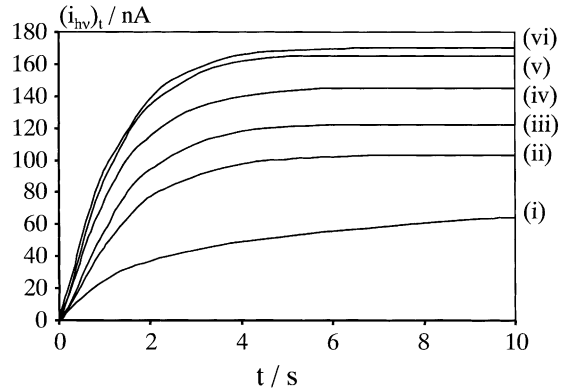

Fig. 9. Light-on current time transient for CdS colloid B at a stationary ODE as a function of $[MV^{2+}]$. $[MV^{2+}] = 0$ (i); 0.99×10^{-4} (ii); 1.98×10^{-4} (iii); 3.38×10^{-4} (iv); 6.98×10^{-4} (v); and $9.09\times10^{-4}\,mol\,m^{-3}$ (vi). [CdS] = $5\,mol\,m^{-3}$.

especially at values of $W < 9\,s^{-1}$. Further, Figs. 8 and 9 show that, under the same conditions, $(i_{hv})_L = (i_{hv})_\infty$ at a given $[MV^{2+}]$. From these observation, Fig. 3 indicates that the system conforms to steady state case A or B. Differentiation between the two cases can be made by consideration of the relative sizes of $X_{k,2}$, X_D and X_ε. In case A, $X_D > X_\varepsilon$, while in case B, $X_D > X_{k,2}$. Given that $D_{MV^{2+}} = 7.2 \times 10^{-10}\,m^2\,s^{-1}$, $X_D = 0.97–5.79 \times 10^{-5}\,m$ over the range of rotation speeds studied in Fig. 8. Spectrophotometric measurements on colloid B show that $X_\varepsilon = 0.37–32 \times 10^{-3}\,m$ over the wavelength range between bandgap and the high energy cut-off of the lamp. Thus, it can be seen that, at all rotation speeds studied, $X_D < X_\varepsilon$. Therefore, by elimination, the data of Figs. 8 and 9 conform to case B and, necessarily, Eq. (4b), indicating that $X_D > X_{k,2}$ and that the photoreduced charge scavenger species are kinetically unstable as they cross the diffusion layer of the ORDE.

Examination of Fig. 3 allows assignment of the transient photocurrent behaviour of Fig. 9 to transient case I_1 or I_2, wherein $(i_{hv})_\infty$ is given by Eq. (8b)/(9b) and Eq. (12) holds. Fig. 10 shows a plot of $(i_{hv})_\infty^{-1}$ versus $[MV^{2+}]^{-1}$ derived from the data of Fig. 9 where assumption 3 is valid. Following the procedure of Fig. 6, and using $k_0 = 0.119\,s^{-1}$ for colloid B (vide supra), a value of k_1' of $1094\,m^3\,mol^{-1}\,s^{-1}$, can be obtained from Fig. 10, which corresponds to $k_1 = 0.995\,s^{-1}$ and $(k_0 + k_1) = 1.114\,s^{-1}$ at $[MV^{2+}] = 9.1 \times 10^{-4}\,mol\,m^{-3}$. It can be shown (Eq. (27) of [3]) that, at short time (typically $t < 1\,s$) the light-on transient photocurrent is given by

$$(i_{hv})_t = FAI_0 \frac{4\phi'\gamma_2\beta}{3\sqrt{\pi}}\tau^{3/2} = \frac{4FAI_0}{3X_\varepsilon}\sqrt{\frac{D_{MV^{2+}}}{\pi}}(k_0 + k_1)\phi' t^{3/2} \quad (14)$$

for all cases of Fig. 2. Fig. 11 shows a plot of $(i_{hv})_t$ versus $t^{3/2}$ for $t < 0.5\,s$ at $[MV^{2+}] = 9.1 \times 10^{-4}\,mol\,m^{-3}$. In accordance with Eq. (14) the slope yields a value of ϕ' of

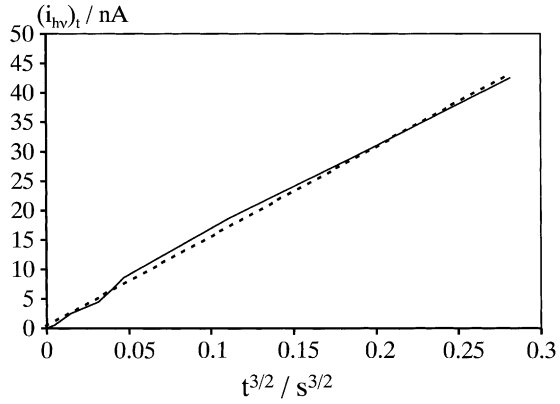

Fig. 11. Plot of $(i_{hv})_t$ vs. $t^{3/2}$ for $t < 0.5\,s$, taken from data of Fig. 9 at $[MV^{2+}] = 9.1 \times 10^{-4}\,mol\,m^{-3}$. Experimental data (unbroken line), regression line (broken line), slope $= 1.52 \times 10^{-7}\,A\,s^{-3/2}$.

0.018, which is in excellent agreement with that obtained under similar conditions from colloid A in the CdS/$Fe(CN)_6^{3-}$ system. Use of Eq. (8b)/(9b) in conjunction with $\phi' = 0.018$ and the $(i_{hv})_\infty$ data of Fig. 9 recorded at $[MV^{2+}] = 9.1 \times 10^{-4}\,mol\,m^{-3}$ then allows calculation of values of $X_{k,2}$ and k_2 of $2.56 \times 10^{-5}\,m$ and $1.094\,s^{-1}$, respectively. As the slowest rotation rate used in these experiments, $1\,s^{-1}$, corresponds to a diffusion layer thickness, X_D, of $5.79 \times 10^{-5}\,m$ for MV^{2+}, this is again suggestive of the majority of the photoreduced charge scavenger species being kinetically unstable as they cross the diffusion layer of the ORDE.

Having obtained k_0, k_1 and k_2, it is now possible to identify which transient case I_1 or I_2, the system conforms to in Fig. 2, and to compare the consequently predicted theoretical transient photocurrent behaviour with that observed experimentally. As in the CdS/$Fe(CN)_6^{3-}$ system, differentiation between cases I_1 and I_2 can be most easily accomplished by consideration of the value of β (see Eq. (6c)) which, using the rate coefficient values determined above, is found to be 1.018 for the CdS/MV^{2+} system at $[MV^{2+}] =$

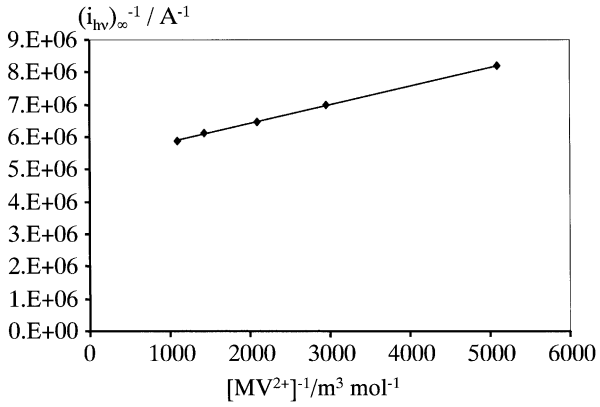

Fig. 10. Reciprocal steady state photocurrent recorded at a stationary ODE, $(i_{hv})_\infty^{-1}$, vs. $[MV^{2+}]^{-1}$, plotted in accordance with Eq. (12) for that data of Fig. 9 recorded under conditions where assumption 3 is valid. $[CdS] = 5\,mol\,m^{-3}$.

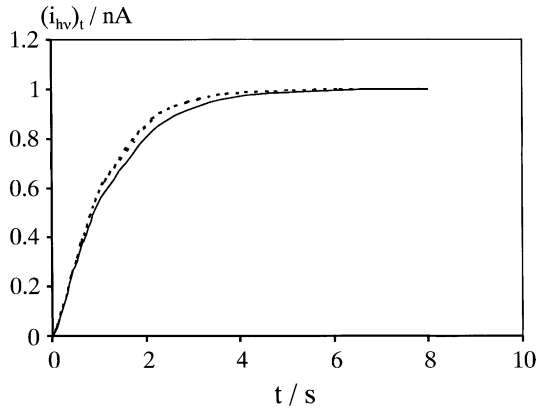

Fig. 12. Matching of experimental data (unbroken line) derived from the light-on transient photocurrent behaviour of CdS colloid B in the presence of MV^{2+} as an electron scavenger, to the theoretical curve (broken line) given by Eq. (13). $[CdS] = 5\,mol\,m^{-3}$; $[MV^{2+}] = 9.1 \times 10^{-4}\,mol\,m^{-3}$.

9.1×10^{-4} mol m^{-3}. Used in conjunction with a calculated mean value of γ_2 of 0.014, this allows the system to be nominally assigned to case I_1. However, calculations again indicate that the derived value of $\beta = 1.018$ is too close to $\beta = 1$ for the approximation given by Eq. (8a) in case I_1 to hold and that, as in the CdS/Fe(CN)$_6^{3-}$ system, the more accurate asymptotic expression given by Eq. (13) provides a closer theoretical description of the experimental time dependence of the light-on photocurrent. The quality of this description can be seen from Fig. 12 which shows both the experimental $(i_{hv})_t$ versus t plot recorded at $[MV^{2+}] = 9.1 \times 10^{-4}$ mol m^{-3} in Fig. 9 and the theoretical plot computed from Eq. (13) using the rate coefficient values derived above.

4. Discussion

As has been suggested previously [2] and by other workers, the surface of the CdS particles employed in this study are characterised by a distribution of inter-band surface states. These particle surface states may be surface S^{2-} ions (as suggested by, inter alia, Kamat and co-workers [34,35] and Baral et al. [36]), sulphur vacancies (V_S, suggested by Duonghong et al. [33]) or some other surface defect. Upon illumination, these defects are oxidised by photogenerated valence band holes, hole capture by S vacancies/S^{2-} ions occurring in 0.2–2 ns [33] and, in the case of S^{2-} ions, with a quantum efficiency of 0.77 [34,35]. As a result of these hole trapping processes, a population of electrons can now survive on the particles due to their corresponding holes being unavailable for the direct recombination reaction. However, these electrons (which themselves reside in shallow electron traps at or near the particle surface, having been captured within 100 fs of their photogeneration [27–30]) can also react with the surface-trapped holes, and it is this indirect recombination reaction that is being interrogated through measurement of k_0.

Table 3 summarises the kinetic parameters obtained for both systems. The values of k_0 for colloids A and B are in excellent agreement with each other and a value of 0.073 ± 0.044 s^{-1} reported previously [2]. The average value of k_0 for the two systems is 0.105 s^{-1} which corresponds to an electron lifetime of 9.5 s, supporting the suggestion that the photogenerated electrons are kinetically stable over the time it takes the illuminated particle to cross the ORDE diffusion layer (it takes a 5 nm particle ~1 s to cross the diffusion layer of an electrode rotating at 16 s^{-1}). Albery et al. [37] report photogenerated electron lifetimes of >10 s when CdS colloids are illuminated in the presence of a hole scavenger such as cysteine. As cysteine plays a role analogous to that of the surface states on CdS particles, the agreement between the two values is not unexpected.

If it is assumed that the particles are roughly spherical, it can be shown that the second-order rate coefficient k_1' is related to the electrochemical rate coefficient for the reaction of the electron scavenger at the particle surface, k_{ET}, by [38]:

$$\frac{1}{k_1'} = \frac{1}{4\pi r_p^2 N_A}\left(\frac{1}{k_{ET}} + \frac{1}{(D_A k_2)^{1/2} + D_A/r_p}\right) \quad (15)$$

where N_A is the Avogadro's constant. Eq. (15) has two limiting forms; that which obtains when interfacial charge-transfer is rate determining:

$$k_1' = 4\pi r_p^2 N_A k_{ET} \quad (16)$$

And that which obtains when mass transfer is rate determining:

$$k_1' = 4\pi r_p^2 N_A \left((D_A k_2)^{1/2} + \frac{D_A}{r_p}\right) \quad (17)$$

Calculated values of k_1' obtained using Eq. (17) are found to be inconsistent with those observed experimentally for the CdS/Fe(CN)$_6^{3-}$ and CdS/MV^{2+} systems, indicating that interfacial charge-transfer is the rate limiting step for both systems. Values of k_{ET} can therefore be calculated using Eq. (16) and are shown in Table 3. The value of 3.12×10^{-6} m s^{-1} obtained for the CdS/MV^{2+} system is broadly in line with that of 0.44×10^{-6} m s^{-1} obtained for the TiO_2/MV^{2+} system [39]. The difference between the two values is a reflection of the fact that the value for the TiO_2 system is reported at the point of zero zeta potential (PZZP) of that material; consequently, there will be no electrostatic factors to affect the electron-transfer rate coefficient. However, the particles in the CdS system, having been prepared in the presence of HMP as a stabilising agent, have a negative surface charge and so are electrostatically attractive to the cationic MV^{2+}, ultimately leading to an enhanced rate of electron-transfer, more than likely through a static charge transfer mechanism, as first established through flash photolysis measurements by Duonghong et al. [33]. The

Table 3
Summary of the physical and kinetic properties of the CdS/Fe(CN)$_6^{3-}$ and CdS/MV^{2+} systems

Parameter	CdS colloid A/Fe(CN)$_6^{3-}$ system	CdS colloid B/MV^{2+} system
$r_p/10^{-9}$ m	12.4	6.8
$D_P/10^{-10}$ m^2 s^{-1}	0.19	0.319
$D_A/10^{-10}$ m^2 s^{-1}	5.859	7.2
E^0(A/A$^-$)/V vs. SCE	0.119	−0.69
k_0/s^{-1}	0.091	0.119
ϕ	0.011[a]	0.012[a]
k_1'/m^3 mol^{-1} s^{-1}	2.029	1094
ϕ'	0.018[b]	0.018[c]
ϕ	0.027[d]	0.020[d]
k_2/s^{-1}	0.101	1.094
k_{ET}/m s^{-1}	1.74×10^{-9}	3.12×10^{-6}

[a] Value calculated from experiments conducted on colloidal CdS in the absence of a deliberately added charge scavenger.
[b] Obtained at $[Fe(CN)_6^{3-}] = 0.0933$ mol m^{-3}.
[c] Obtained at $[MV^{2+}] = 9.1 \times 10^{-4}$ mol m^{-3}.
[d] Value calculated from Eq. (2b), k_0, k_1 and values of ϕ' obtained from experiments conducted on CdS in the presence of a deliberately added charge scavengers Fe(CN)$_6^{3-}$ or MV^{2+}.

opposite effect can be seen to operate in the case of the CdS/$Fe(CN)_6^{3-}$ system wherein the expected anion/particle Coulombic repulsion should cause electron-transfer to occur through a predominantly dynamic charge transfer mechanism and results in a value of k_{ET} three orders of magnitude less than that obtained for the CdS/MV^{2+} system.

A qualitatively similar, but quantitatively less extreme, trend can be seen in the values of k_2, suggesting that the loss reactions for the photoreduced electron scavengers are oxidation of $Fe(CN)_6^{4-}$ and $MV^{+\bullet}$ by photogenerated holes on the particles. At this point, it is difficult to say for certain whether the holes participating in such an oxidation reside in the particle valence band or oxidised S vacancies/S^{2-} sites on the particle surface; however, that hole trapping from the valence band by surface states occurs on the ns timescale, while scavenger reoxidation occurs s timescale, is strongly suggestive of the participation of oxidised surface states.

As has been defined previously [25], in the case of colloidal semiconductors ϕ (the quantum efficiency for photogeneration of S^* in reaction (Ia)/(IIa)) corresponds to the photogeneration of holes that react in such a fashion as to be unavailable for direct recombination processes, so leaving stable photogenerated electrons on the particles (whether in the conduction band or shallow traps at or near the surface, vide supra). ϕ is then given by

$$\phi = \frac{\sum_i k_i [T_h]_i [h^+_{VB}]}{\sum_i k_i [T_h]_i [h^+_{VB}] + k_{R1}[e^-_{CB}][h^+_{VB}] + k_{R2}[e^-_T][h^+_{VB}]} \quad (18)$$

where k_i, k_{R1}, k_{R2} are the rate coefficients for the reactions of valence band holes with hole traps, T_h, of type i, conduction band electrons (concentration given by $[e^-_{CB}]$) and photogenerated electrons in shallow traps at or near the particle surface (concentration given by $[e^-_T]$). From Table 3, it can be seen that the average value of ϕ calculated from experiments conducted on colloidal CdS in the absence of a deliberately added charge scavenger is 0.0105 indicating that the dominant reaction for photogenerated electrons is recombination with valence band holes and that those surviving to reach the electrode do so because corresponding holes have been lost to particle corrosion reactions or trace adventitious electron donors. Table 3 also shows values of ϕ calculated from Eq. (2b), k_0, k_1 and values of ϕ' obtained from experiments conducted on CdS in the presence of a deliberately added charge scavengers $Fe(CN)_6^{3-}$ or MV^{2+}. The values obtained, 0.027 and 0.02 for the CdS/$Fe(CN)_6^{3-}$ and CdS/MV^{2+} systems, respectively, are in fair agreement with each other and approximately twice those obtained in the absence of charge scavengers. This modest increase can be understood by consideration of Eq. (18). Given that it is now widely held that the dominant process in these systems is electron hole recombination, Eq. (18) could be written as

$$\phi = \frac{\sum_i k_i [T_h]_i}{k_{R1}[e^-_{CB}] + k_{R2}[e^-_T]} \quad (19)$$

indicating that a possible source of the observed increase in ϕ upon introduction of electron scavengers is a decrease in either $[e^-_{CB}]$ or $[e^-_T]$.

5. Conclusions

The ORDE is a powerful tool for the interrogation of dynamic particle-to-electrode and particle-to-charge scavenger electron-transfer. Interrogation of the two model particle/scavenger systems, CdS/$Fe(CN)_6^{3-}$ and CdS/MV^{2+} with the ORDE allows for the determination of the relative sizes of X_D, $X_{k,2}$ and X_ε for each system with subsequent calculation of ϕ, k_0, k'_1, k_2 and k_{ET}. Values are given in Table 3. The value of k_0 supports the assumption that the charge carrier loss process interrogated by transient photocurrent measurements on particles in the absence of an electron scavenger is not direct photogenerated electron–valence band hole recombination but loss of electrons left on the particles after some valence band hole filling reaction has occurred. This reaction is the filling of the holes by electrons originating from inter-band surface states. The values of k'_1 and k_{ET} for the two particle scavenger systems underline the importance of Coulombic interaction between particle and scavenger in determining the efficiency of particle-to-scavenger electron-transfer. The back reaction of the photoreduced electron scavenger is reoxidation by holes trapped (most probably) on the surface of the photoexcited particles. The relative sizes of k_2 for the two systems indicates that, unless the charge on the scavenger is neutralised or reversed during the process associated with k_1, then those Coulombic interactions that work in favour of the desirable particle-to-scavenger electron-transfer event also promote the undesirable scavenger-to-particle back reaction. Indeed, it would appear that the system that ultimately gives rise to the highest photocurrent, and thus yield of photoreduced scavenger, is that for which the rate coefficient for the back reaction is lowest, i.e. the CdS/$Fe(CN)_6^{3-}$ system. This indicates that k_2 plays a key role in determining overall process efficiency, an observation that has far-reaching implications for the design of CdS-based photocatalytic systems.

Acknowledgements

The author wishes to thank Andrew Mills for the invitation to submit this paper, and Peter K.J. Robertson and Jason Riley for helpful discussions. He would also like to thank W. John Albery for initiating the line of enquiry that ultimately led to the results presented above.

References

[1] C. Boxall, W.J. Albery, Phys. Chem. Chem. Phys. 2 (2000) 3631.
[2] C. Boxall, W.J. Albery, Phys. Chem. Chem. Phys. 2 (2000) 3641.

[3] C. Boxall, W.J. Albery, Phys. Chem. Chem. Phys. 2 (2000) 3651.
[4] C. Boxall, Chem. Soc. Rev. 23 (1994) 137.
[5] A. Fujishima, T.N. Rao, D.A. Tyrk, J. Photochem. Photobiol. C 1 (2000) 1.
[6] D.F. Ollis, H. Al-Ekabi (Eds.), Photocatalytic Purification and Treatment of Water and Air, Elsevier, Amsterdam, 1993.
[7] G.R. Helz, R.G. Zepp, D.G. Crosby (Eds.), Aquatic and Surface Photochemistry, CRC Press, Boca Raton, FL, 1993.
[8] M.R. Hoffman, S.T. Martin, W. Choi, D. Bahnemann, Chem. Rev. 95 (1995) 69.
[9] M.M. Halmann, Photodegradation of Water Pollutants, CRC Press, Boca Raton, FL, 1996.
[10] A. Mills, S. Le Hunte, J. Photochem. Photobiol. A 108 (1997) 1.
[11] R.A. Mackay, J. Texter (Eds.), Electrochemistry in Colloids and Dispersions, VCH, New York, 1992.
[12] P. Kamat, Chem. Rev. 93 (1993) 267.
[13] P. Kamat, Prog. React. Kinet. 19 (1994) 277.
[14] A. Henglein, Chem. Rev. 89 (1989) 1861.
[15] M.L. Steigerwald, L.E. Brus, Acc. Chem. Res. 23 (1990) 183.
[16] Y. Wang, N. Herron, J. Phys. Chem. 95 (1991) 525.
[17] H. Weller, Adv. Mater. 5 (1993) 88.
[18] A. Hagfeldt, M. Grätzel, Chem. Rev. 95 (1995) 49.
[19] S.N. Frank, A.J. Bard, J. Phys. Chem. 81 (1977) 1484.
[20] M. Heyrovsky, J. Jirkovsky, Langmuir 11 (1995) 4288.
[21] M. Heyrovsky, J. Jirkovsky, B.R. Müller, Langmuir 11 (1995) 4293.
[22] M. Heyrovsky, J. Jirkovsky, M. Struplová-Bartácková, Langmuir 11 (1995) 4300.
[23] M. Heyrovsky, J. Jirkovsky, M. Struplová-Bartácková, Langmuir 11 (1995) 4309.
[24] W.J. Albery, P.N. Bartlett, J.D. Porter, J. Electrochem. Soc. 131 (1984) 2892.
[25] W.J. Albery, P.N. Bartlett, J.D. Porter, J. Electrochem. Soc. 131 (1984) 2896.
[26] N. Buhler, K. Meier, J.F. Reber, J. Phys. Chem. 88 (1984) 3261.
[27] D.E. Skinner, D.P. Colombo Jr., J.J. Cavaleri, R.M. Bowman, J. Phys. Chem. 99 (1995) 7853.
[28] J.Z. Zhang, R.H. O'Neil, T.W. Roberti, J.L. McGowen, J.E. Evans, Chem. Phys. Lett. 218 (1994) 479.
[29] J.Z. Zhang, R.H. O'Neil, T.W. Roberti, Appl. Phys. Lett. 64 (1994) 1989.
[30] J.E. Evans, K.W. Springer, J.Z. Zhang, J. Chem. Phys. 101 (1994) 6222.
[31] W.J. Albery, M.D. Archer, R.G. Egdell, J. Electroanal. Chem. 82 (1977) 199.
[32] W.J. Albery, W.R. Bowen, F.S. Fisher, A.D. Turner, J. Electroanal. Chem. 107 (1980) 11.
[33] D. Duonghong, J. Ramsden, M. Grätzel, J. Am. Chem. Soc. 104 (1982) 2977.
[34] P.V. Kamat, K.R. Gopidas, N.M. Dimitrijevic, Mol. Cryst. Liq. Cryst. 183 (1990) 439.
[35] P.V. Kamat, T.W. Ebbesen, N.M. Dimitrijevic, A.J. Nozik, Chem. Phys. Lett. 157 (1989) 384.
[36] S. Baral, A. Fojtik, H. Weller, A. Henglein, J. Am. Chem. Soc. 108 (1986) 375.
[37] W.J. Albery, G.T. Brown, J.R. Darwent, E. Saievar-Iranizad, J. Chem. Soc., Faraday Trans. I 81 (1985) 1999.
[38] W.J. Albery, P.N. Bartlett, J. Electroanal. Chem. 131 (1982) 137.
[39] G.T. Brown, J.R. Darwent, J. Chem. Soc., Chem. Commun. (1985) 98.